Phytopathology Research

RESEARCH

Open Access

# GmPAO-mediated polyamine catabolism enhances soybean *Phytophthora* resistance without growth penalty

Kun Yang[1], Qiang Yan[1,2], Yi Wang[1], Hao Peng[3], Maofeng Jing[1] and Daolong Dou[1*]

## Abstract

Plant immunity is activated upon perception of pathogens and often affects growth when it is constitutively active. It is still a challenge to balance plant immunity and growth in disease resistance breeding. Here, we demonstrated that soybean (*Glycine max*) polyamine oxidase (GmPAO) confers resistance to multiple *Phytophthora* pathogens, but has no obvious adverse impact on agronomic traits. GmPAO produces $H_2O_2$ by oxidizing spermidine and spermine. *Phytophthora sojae* induces an increase in these two substrates, and thus promotes GmPAO-mediated polyamine catabolism specifically during infection. Interestingly, we found that the two substrates showed higher accumulation in transgenic soybean lines overexpressing *GmPAO* than in WT and CK after inoculation with *P. sojae* to ensure $H_2O_2$ production during infection, rather than directly inhibit *P. sojae*. In these transgenic soybean plants, the significantly enhanced resistance to different *P. sojae* isolates was achieved; PAMP-induced $H_2O_2$ accumulation was enhanced by *GmPAO* overexpression. Moreover, transient expression of *GmPAO* also significantly improved *Nicotiana benthamiana* resistance to *Phytophthora capsici* and *Phytophthora parasitica* in agroinfiltration assays. Our results provide a novel approach to allow rapid defense responses in plants upon pathogen infection while minimizing growth penalties under normal conditions, with a clear mechanism in which plant promotes $H_2O_2$ production via pathogen-activated substrates.

**Keywords:** Genetic engineering, Disease resistance, Hydrogen peroxide, *Phytophthora*, Polyamine oxidase, Soybean

## Background

The oomycete genus *Phytophthora,* which consists of nearly 200 described species, has been and continues to be a significant threat to global agroecosystems and food security (Kamoun et al. 2015; Wang et al. 2020). For example, *Phytophthora sojae* in soybean causes 'damping off' at the seedling stage and root rot in adult plants, resulting in an annual loss of $1–2 billion worldwide (Zhou et al. 2021). Another prevalent phytopathogenic oomycete, *P. capsica*, is a highly dynamic and destructive pathogen attacking vegetables, including cucurbit, pepper, tomato, eggplant, lima bean, etc. (Lamour et al. 2012; Li et al. 2019b). Furthermore, *P. parasitica* causes notable diseases of brown rot, foot rot, and black shank in tobacco, affecting almost all tobacco growing areas worldwide with losses as high as 100% (Panabieres et al. 2016; Yu et al. 2020). Accordingly, plants respond to pathogen infection using an efficient, dynamic, and hierarchical immune system (Jones and Dangl 2006; Wang et al. 2020). Immune activation in plants confers resistance against invading pathogens, but constitutive immune responses are costly and impede plant growth and environmental fitness (Deng et al. 2020). Therefore, a delicate balance between warding off potential pathogens

*Correspondence: ddou@njau.edu.cn

[1] Key Laboratory of Plant Immunity, College of Plant Protection, Academy for Advanced Interdisciplinary Studies, Nanjing Agricultural University, Nanjing 210095, China
Full list of author information is available at the end of the article

and avoiding negative impacts on growth fitness must be maintained (Ning et al. 2017; Gao et al. 2021). Genetic engineering is a desirable approach to solve these problems via expression of carefully selected genes (Deng et al. 2020; Liu et al. 2021).

So far, some emerging breeding approaches for crop disease resistance have been extensively studied, including (1) molecular strategies for enhancing plant immune system (Frailie and Innes 2021); (2) modification of plant susceptibility genes (Tian et al. 2020; Koseoglou et al. 2022); (3) engineering antimicrobial proteins (Sinha and Shukla 2019; Liu et al. 2021); (4) interfering with pathogenicity (Li et al. 2021); and (5) manipulation of the expression of 'master-switch' genes, such as kinases, transcription factors, and signal molecules (Ma et al. 2017; Wang et al. 2018; Narvaez et al. 2020; Liu et al. 2021). At the same time, several strategies have been developed to manipulate the expression of 'master-switch' genes. For example, uORFs-mediated translational control of *Arabidopsis NPR1* generated broad-spectrum resistance without the NPR1-induced growth penalty in transgenic rice (Xu et al. 2017). Balancing yield and immunity has also been greatly achieved. For example, a rice locally adaptive *ROD1* allele confers higher basal resistance without loss of crop yield (Gao et al. 2021), whereas IPA1 promotes both yield and disease resistance by sustaining a balance between growth and immunity (Wang et al. 2018).

Dissection of plant–pathogen interactions at molecular level uncovers potential engineering targets for plant defense enhancement. As is well known, hydrogen peroxide ($H_2O_2$) is a critical signal triggering plant defense response and can be rapidly produced under biotic stresses (Qi et al. 2018). Plant polyamines (PAs) are involved in immunity against pathogens, notably by amplifying pattern-triggered immunity (PTI) responses through the production of $H_2O_2$ (Gerlin et al. 2021). $H_2O_2$ can be generated via spermidine (Spd) and spermine (Spm) oxidation catalyzed by PA oxidase (PAO) (Gerlin et al. 2021). Although previous studies found that overexpression of PAO can improve disease resistance in model plants *Arabidopsis* (Mo et al. 2015) and tobacco (Moschou et al. 2009), no transgenic application of PAO-encoding genes in crops has been reported.

Here, we aim to improve *Phytophthora* resistance in soybean by overexpressing its native *PAO* (*GmPAO*) gene that oxidizes Spd and Spm to generate $H_2O_2$. We demonstrated that the two substrates, Spd and Spm, were significantly increased upon *P. sojae* infection. Transgenic soybean lines overexpressing *GmPAO* gene exhibited higher $H_2O_2$ production only in response to *P. sojae* infection. The elevated PTI activation was also observed in the *GmPAO* overexpression soybean lines. Moreover, Spd and Spm contents were highly induced in these transgenic lines. As expected, the transgenic soybean lines confer disease resistance to *P. sojae* without growth penalty. Thus, we propose a method by expressing plant *PAO* genes to induce disease resistance while minimizing cellular damage caused by $H_2O_2$.

## Results

### Spd and Spm contents are increased in soybean after infection with *P. sojae*

The major polyamines (PAs) in plants are the diamine putrescine (Put), the triamine spermidine (Spd), and the tetraamine spermine (Spm) (Seifi and Shelp 2019). As PAs have an important role in the interaction between plants and pathogens (Gerlin et al. 2021), we determined to investigate PA changes in soybean plants in response to *P. sojae* infection using ultra-high-performance liquid chromatography coupled to quadrupole Orbitrap high-resolution mass spectrometry (UHPLC-MS) method. The results showed that the Put content in soybean was significantly decreased during *P. sojae* infection (Fig. 1a). In contrast, the Spd content was significantly increased to 3.0-fold at 16 h post-inoculation (hpi), 2.0-fold at 32 hpi, and 1.6-fold at 48 hpi (Fig. 1a). Furthermore, the Spm content in soybean was increased to 1.4-fold at 16 hpi, 2.0-fold at 32 hpi, and 1.3-fold at 48 hpi (Fig. 1a). Collectively, the results suggest that the Spd and Spm contents in soybean were increased during *P. sojae* infection.

### Transgenic soybean lines overexpressing *GmPAO* gene display significantly boosting hydrogen peroxide production at infection sites

We cloned the full-length cDNA sequence of *GmPAO* (Glyma.09G227500.1) according to the genome sequence of *Glycine max* Wm82.a2.v1 in the Phytozome database, and generated stable transgenic soybean lines overexpressing *GmPAO* gene. Two independent transgenic soybean lines (T1-1 and T1-4-1) overexpressing *GmPAO* were generated and characterized by molecular screening at the T5 generation (Additional file 1: Figure S1 and Additional file 2: Table S1). T1-1-1, T1-1-3, T1-1-4, and T1-1-5 sublines were all derived from T1-1. To further confirm the expression of *GmPAO* in the transgenic lines, we detected the PAO enzymatic activity. The results showed that the PAO enzymatic activity in transgenic soybean lines was increased to ~ 1.8-fold compared with that in WT and the non-*GmPAO* transgenic line (CK) in the absence of *P. sojae* challenge (Fig. 1b). Furthermore, we also detected the PAO enzymatic activity during *P. sojae* infection. The results showed that the PAO enzymatic activity in transgenic soybean lines was increased to 2.5-fold at 16 hpi, and 1.8-fold at both 32 and 48 hpi compared with that in WT and CK (Fig. 1b). Thus, in comparison with WT and CK, all the *GmPAO*

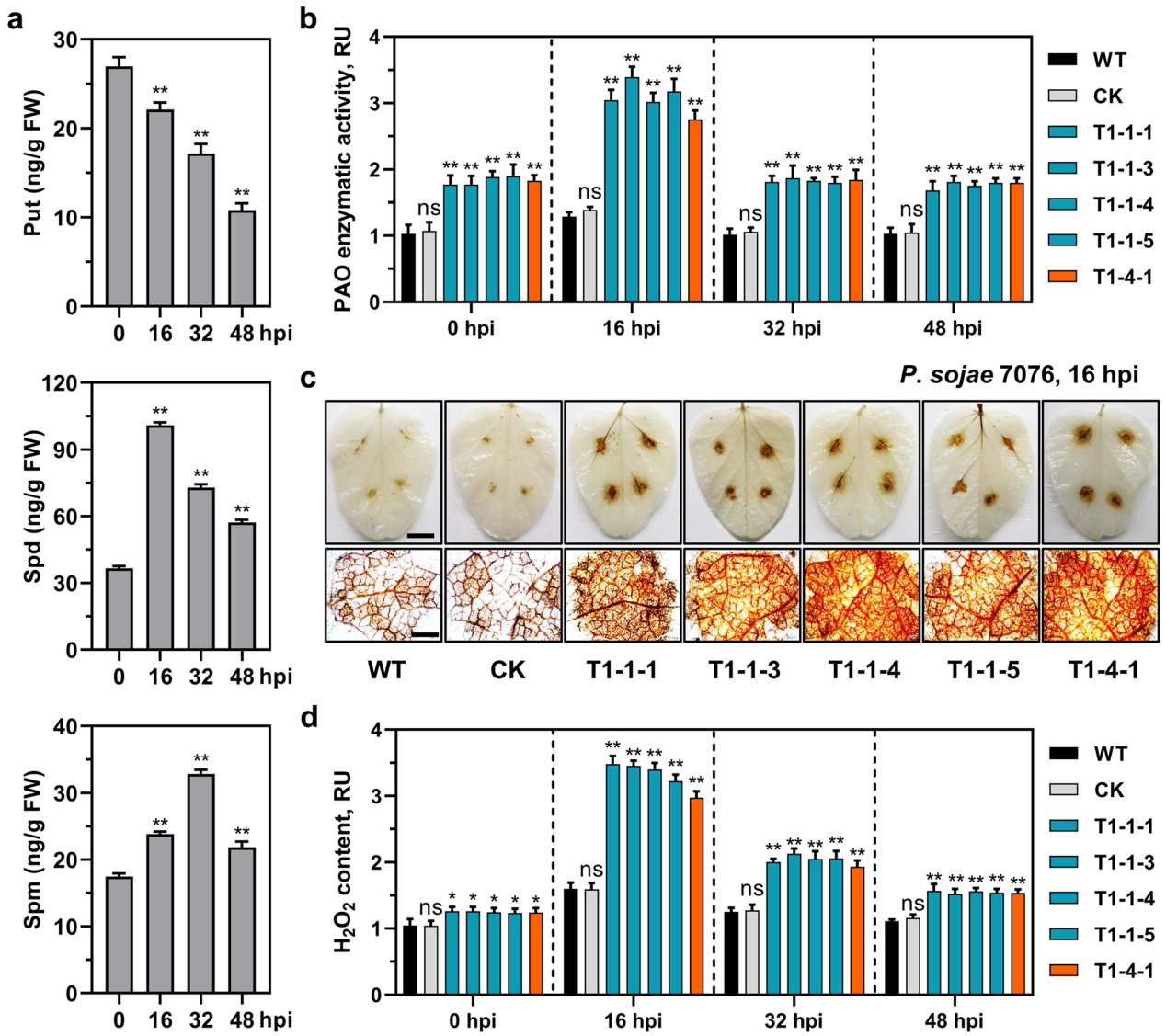


**Fig. 1** Transgenic soybean lines overexpressing *GmPAO* display significantly boosting $H_2O_2$ production at the *P. sojae* infection sites. WT: wild-type soybean cultivar Williams 82; CK: non-*GmPAO* transgenic soybean line. T1-1 (including T1-1-1, T1-1-3, T1-1-4, and T1-1-5) and T1-4-1 are progenies of two independent transgenic soybean lines overexpressing *GmPAO* gene. **a** Changes in the contents of putrescine (Put), spermidine (Spd), and spermine (Spm) in WT plants in response to *P. sojae* infection. Error bar represents mean ± SD, n = 3, n represents sample number. **b**, **d** PAO enzymatic activity and $H_2O_2$ content in transgenic soybean plants during *P. sojae* infection. RU: relative activity units (Error bar represents mean ± SD, n = 3, n represents sample number). **c** DAB staining of $H_2O_2$ at 16 hpi. Scale bar: 1 cm (upper). Micrograph of DAB staining at *P. sojae* infection sites. Scale bar: 20 μm (lower). All the experiments were performed three times (biological replicates) with similar results. The data in **a, b,** and **d** were analyzed by Shapiro–Wilk test to determine the Normality and Lognormality Tests across groups, and then analyzed by one-way ANOVA with post-hoc Dunnett's multiple comparisons test for groups that had passed the normality test (ns, no significant difference; $^*P < 0.05$; $^{**}P < 0.01$). The exact n, SD values, and *P* values are shown in the data

overexpression soybean lines showed significantly enhanced polyamine synthetic capacity before and after *P. sojae* infection, with the highest PAO enzymatic activity being detected at 16 hpi.

To monitor the effect of GmPAO-mediated polyamine catabolism, we conducted a series of experiments to test $H_2O_2$ production. First, we investigated $H_2O_2$ accumulation in the transgenic soybean lines using 3,3′-diaminobenzidine (DAB) staining assay (Wang et al. 2020; Zhou et al. 2021). Compared with WT and CK, the five transgenic soybean lines showed significantly enhanced $H_2O_2$ accumulation at 16 hpi (Fig. 1c). Interestingly, we

found that $H_2O_2$ accumulation occurred only at the *P. sojae* infection sites, on the contrary, there was no $H_2O_2$ accumulation at the *P. sojae* no-infection sites (Fig. 1c). These results preliminarily indicated that GmPAO-mediated $H_2O_2$ generation is activated upon *P. sojae* infection. $H_2O_2$ production is not only required in many important defense reactions (Qi et al. 2018) but also inevitable results of oxidative damage (Mittler 2017; Kerchev and Van Breusegem 2022). Intriguingly, GmPAO-mediated $H_2O_2$ accumulation only occurred at the *P. sojae* infection sites to minimize cellular damage caused by $H_2O_2$.

Second, we examined the relative $H_2O_2$ levels in WT, CK and transgenic soybean plants using $H_2O_2$ assay kit (Yin et al. 2018; Zhang et al. 2019a). The results showed that the $H_2O_2$ content in transgenic soybean lines was only weakly increased to 1.2-fold compared with that in WT and CK in the absence of *P. sojae* challenge (Fig. 1d), indicating a relatively normal $H_2O_2$ level in the transgenic soybean lines under normal conditions. We further detected the relative $H_2O_2$ level during *P. sojae* infection. The results showed that the relative $H_2O_2$ level in the transgenic soybean lines was increased to 2.3-fold at 16 hpi, 1.7-fold at 32 hpi, and 1.4-fold at 48 hpi compared with that in WT and CK (Fig. 1d). These results further indicated that GmPAO-mediated $H_2O_2$ is activated upon *P. sojae* infection.

Together, the results indicated that Spd/Spm contents in soybean plants were upregulated in response to *P. sojae* infection, and GmPAO-mediated Spd/Spm catabolism promoted $H_2O_2$ production mostly at the *P. sojae* infection sites.

#### GmPAO promotes PAMP-induced $H_2O_2$ accumulation

PAs are involved in PTI responses (Gerlin et al. 2021). We therefore investigated the effect of GmPAO on the pathogen-associated molecular patterns (PAMP)-induced reactive oxygen species (ROS) burst using an L-012 based assay (Pi et al. 2022). We examined the well-known bacterial pattern flg22-induced ROS and found that there was a significantly enhanced ROS production in the transgenic soybean lines (Fig. 2a). Chitin-induced ROS accumulation was also enhanced by GmPAO (Fig. 2b). Next, we validated the regulation activity of flg22/chitin-induced ROS accumulation by GmPAO using a transient expression assay in *Nicotiana benthamiana*. Consistent with the results in transgenic soybean lines, the transient expression of *GmPAO* in *N. benthamiana* enhanced flg22/chitin-induced ROS accumulation (Fig. 2c, d). These results suggest that GmPAO can promote flg22/chitin-induced $H_2O_2$ accumulation.

#### Transgenic soybean lines overexpressing *GmPAO* gene display significantly elevated contents of Spd and Spm when challenged by *P. sojae*

To investigate the effect of GmPAO-mediated polyamine catabolism, we measured the contents of PAs in transgenic soybean lines upon infection by *P. sojae*. The results showed that there was no significant change in Spd content among the transgenic soybean lines, WT, and CK in the absence of *P. sojae* challenge (Fig. 3a). Furthermore, we detected the Spd content during *P. sojae* inoculation. The results showed that the Spd content in transgenic soybean lines was increased to 1.7-fold at 16 hpi, 1.5-fold at 32 hpi, and 1.3-fold at 48 hpi compared with that in WT and CK (Fig. 3a). Thus, in comparison with WT and CK, all *GmPAO* overexpression soybean lines showed significantly elevated Spd content after *P. sojae* infection.

We also measured Spm content in the transgenic soybean lines. Consistent with Spd, there was no difference in Spm content among the transgenic soybean lines, WT, and CK in the absence of *P. sojae* challenge (Fig. 3b). The Spm content in transgenic soybean lines was increased to 1.7-fold, 3.4-fold, and 4.0-fold compared with that of WT and CK at 16, 32, and 48 hpi, respectively (Fig. 3b). Upon *P. sojae* inoculation, all soybean plants overexpressing *GmPAO* showed a higher accumulation of Spd and Spm as compared to WT and CK.

#### Spd and Spm inhibit colony growth, zoospore germination, and pathogenicity of *P. sojae* at high concentrations

Spd and Spm are reported to significantly inhibit conidial proliferation and colony growth of *Verticillium dahliae* (Mo et al. 2015). To investigate the roles of Spd and Spm during *P. sojae* infection, we evaluated whether Spd and Spm have inhibitory effects on *P. sojae*. The application of Spd at 0.7 and 0.8 mg/mL significantly inhibited colony growth in vitro, with application at 0.9 mg/mL fully inhibiting colony growth of *P. sojae* (Fig. 4a, b). And the application of Spm at 0.2 and 0.3 mg/mL significantly inhibited colony growth in vitro, with application at 0.4 mg/mL extremely inhibiting colony growth (Fig. 4a, b). Of the two PAs tested, Spm displayed a higher *P. sojae* inhibition activity. Further experiments showed that Spd and Spm could efficiently inhibit zoospore germination (Fig. 4c, d). Spd and Spm also significantly inhibited *P. sojae* pathogenicity (Additional file 1: Figure S2). Together, these results indicated that high concentrations of Spd and Spm could directly inhibit *P. sojae*, but the concentrations of Spd and Spm in transgenic lines were far below the inhibitory concentrations. Thus, the increased Spd and Spm in the *GmPAO* overexpression soybean lines may ensure $H_2O_2$ accumulation during infection.

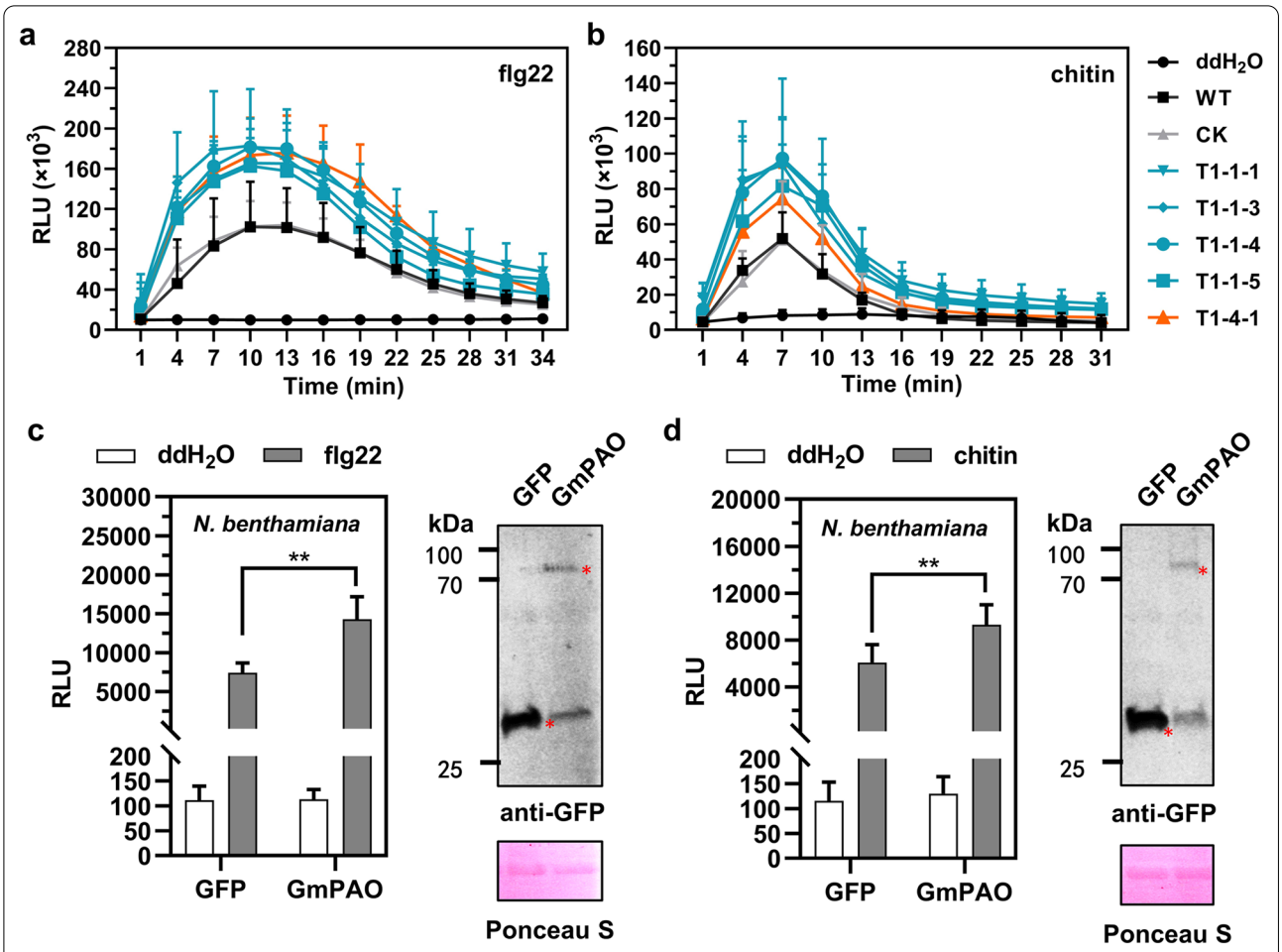


**Fig. 2** GmPAO promotes PAMP (flg22 or chitin)-induced $H_2O_2$ accumulation. **a**, **b** GmPAO promoted PAMP (flg22 or chitin)-induced $H_2O_2$ accumulation in transgenic soybean lines. The leaves (2-week-old) were subjected to flg22- (**a**) or chitin-induced (**b**) ROS examination, and the relative luminescence unit (RLU) value was recorded. Error bar represents mean ± SD, n ≥ 8, n represents sample number. **c**, **d** GmPAO promoted PAMP (flg22 or chitin)-induced $H_2O_2$ accumulation in *N. benthamiana*. The indicated constructs were transiently expressed by *Agrobacterium*-mediated transient expression for 2 days and subjected to flg22- (**c**) or chitin-induced (**d**) ROS examination. GFP was used as a control. The protein expression is shown in the right panel. Error bar represents mean ± SD, n = 8, n represents sample number. All the experiments were performed three times (biological replicates) with similar results. The data were analyzed by Shapiro–Wilk test to determine the Normality and Lognormality Tests across groups, and then analyzed by unpaired *t* test for groups that had passed the normality test (**$P < 0.01$). The exact n, SD values, and *P* values are shown in the data

### GmPAO significantly enhances resistance against *P. sojae* in the transgenic soybean lines

To test whether the *GmPAO* overexpression soybean lines are resistant to *P. sojae*, we challenged these soybean lines with two representative virulent *P. sojae* isolates (P7076 and PS14) that belong to distinct genetic clades (Zhang et al. 2019b). First, etiolated hypocotyls were inoculated with equal amounts of mycelia. The results showed that compared with WT and CK, all the *GmPAO* overexpression lines exhibited significantly reduced lesion length (Fig. 5a, d and Additional file 1: Figure S3) and *P. sojae* biomass accumulations in hypocotyls (Fig. 5f) after inoculation with either P7076 or PS14. The results preliminarily indicated that all these transgenic soybean lines exhibited substantially enhanced resistance against two *P. sojae* isolates when compared with WT and CK.

Second, the soybean leaves were inoculated with equal amounts of mycelia. Compared with WT and CK, all the *GmPAO* overexpression lines also showed a significant reduction in both lesion size (Fig. 5b, e and Additional file 1: Figure S4) and *P. sojae* biomass accumulation in leaves (Fig. 5g) after inoculation with either P7076 or PS14. These results also indicated that all these transgenic soybean lines exhibited substantially enhanced resistance compared with WT and CK.

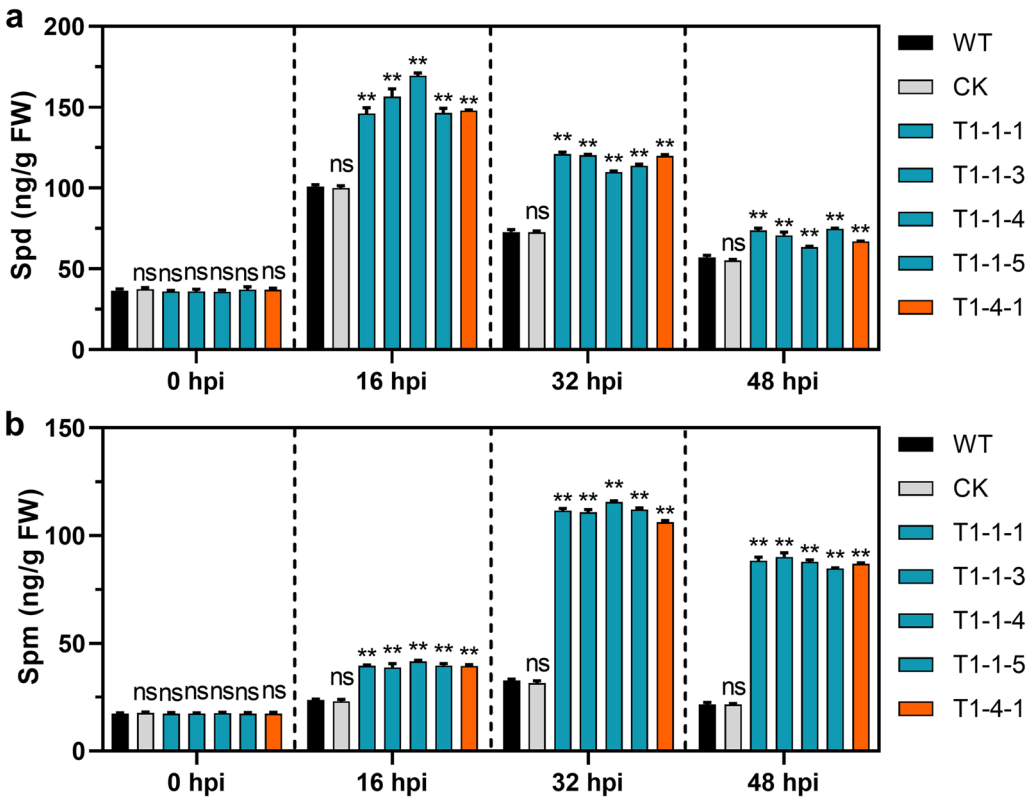


**Fig. 3** Changes in the contents of Spd (**a**) and Spm (**b**) in transgenic soybean lines upon *P. sojae* inoculation. Error bar represents mean ± SD, n = 3, n represents sample number. All the experiments were performed three times (biological replicates) with similar results. The data were analyzed by Shapiro–Wilk test to determine the Normality and Lognormality Tests across groups, and then analyzed by one-way ANOVA with post-hoc Dunnett's multiple comparisons test for groups that had passed the normality test (ns, no significant difference; $^{**}P < 0.01$). The exact n, SD values, and *P* values are shown in the data

Third, since *P. sojae* infects roots in the field, we performed a root-dipping inoculation experiment to further evaluate the resistance. Consistent with the results of etiolated hypocotyl and leaf inoculation, all the *GmPAO* overexpression lines showed enhanced resistance against *P. sojae* when compared with WT and CK (Fig. 5c, h and Additional file 1: Figure S5). At 12 days post-inoculation (dpi), more than half of the *GmPAO* overexpression plants exhibited healthy growth, whereas about 80% of WT and CK plants were killed by the pathogen (Fig. 5c, h and Additional file 1: Figure S5). Collectively, these results further indicated that the *GmPAO* overexpression soybean lines exhibited substantially enhanced resistance compared with WT and CK.

### GmPAO enhances resistance to *P. capsici* and *P. parasitica* in *N. benthamiana*

To investigate whether the resistance conferred by GmPAO is broad-spectrum and effective to other *Phytophthora* pathogens, we infiltrated *Agrobacterium tumefaciens* cells carrying a GFP or GmPAO fusion construct and then inoculated the infiltrated leaves with *P. capsici*. The lesion diameters were measured at 36 and 48 hpi. Interestingly, compared with the *GFP* expression control, the leaves expressing *GmPAO* exhibited a significant reduction in *P. capsici* colonization (Fig. 6a, b). Consistent with reduced lesion size, *P. capsici* biomass was also less in *GmPAO*-expressing leaves than in the *GFP*-expressing control (Fig. 6c). Western blot analysis indicated that all the recombinant proteins were properly expressed at expected sizes in *N. benthamiana* (Fig. 6d). These results indicated that *GmPAO* enhanced *N. benthamiana* resistance against *P. capsici* when overexpressed *in planta*.

Furthermore, *GFP* and *GmPAO* were transiently expressed in *N. benthamiana* leaves individually and were subsequently challenged with *P. parasitica*. The results indicated that GmPAO also significantly improved *N. benthamiana* resistance against *P. parasitica* (Fig. 6e–h) in agroinfiltration assays, demonstrating its effectiveness in conferring broad-spectrum *Phytophthora* resistance. Collectively, these results indicated that

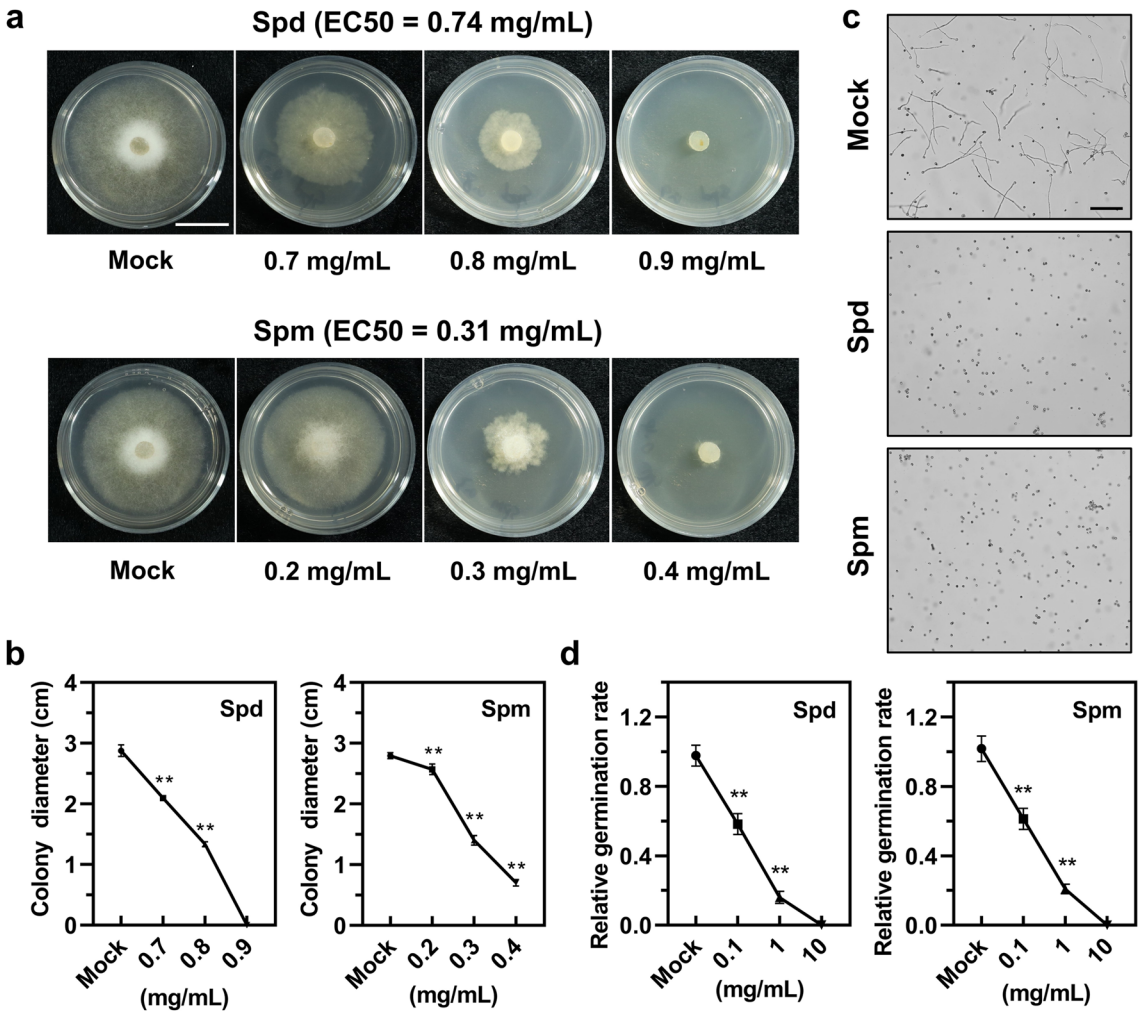


**Fig. 4** Effects of PAs (Spd and Spm) on colony growth and zoospore germination of *P. sojae*. **a** Inhibition of *P. sojae* hyphal growth by Spd or Spm. Mock represents treatment with $ddH_2O$. Scale bar, 1 cm. **c** Inhibition of *P. sojae* zoospore germination by Spd (1 mg/mL) or Spm (1 mg/mL). Mock represents treatment with $ddH_2O$. Scale bar, 50 μm. **b**, **d** Statistics of colony diameters and zoospore germination rates of *P. sojae*. Error bar represents mean ± SD, n = 8, n represents sample number. All the experiments were performed three times (biological replicates) with similar results. The data were analyzed by Shapiro–Wilk test to determine the Normality and Lognormality Tests across groups, and then analyzed by one-way ANOVA with post-hoc Dunnett's multiple comparisons test for groups that had passed the normality test (**$P < 0.01$). The exact n, SD values, and *P* values are shown in the data

GmPAO-mediated polyamine catabolism significantly enhanced plant broad-spectrum resistance to *Phytophthora* pathogens.

### Transgenic soybean lines exhibit no changes in agronomic traits

In crops, genetic immunity to disease often associates with an unintended reduction in growth and yield (Ning et al. 2017). Therefore, we performed detailed agronomic trait tests on these transgenic plants. We first examined the effect of overexpression of *GmPAO* on morphology, and found that the transgenic lines exhibited no apparent changes in morphology, including growth phenotype, pod, and seed compared with WT and CK (Fig. 7a). We next examined the effect on seed weight and germination rate, and found that there were no significant differences in 100-seed weight and germination rate among the transgenic lines, WT, and CK (Fig. 7b, c). Taken together, we demonstrated that GmPAO confers resistance to multiple *Phytophthora* pathogens, and no adverse impact on agronomic traits.

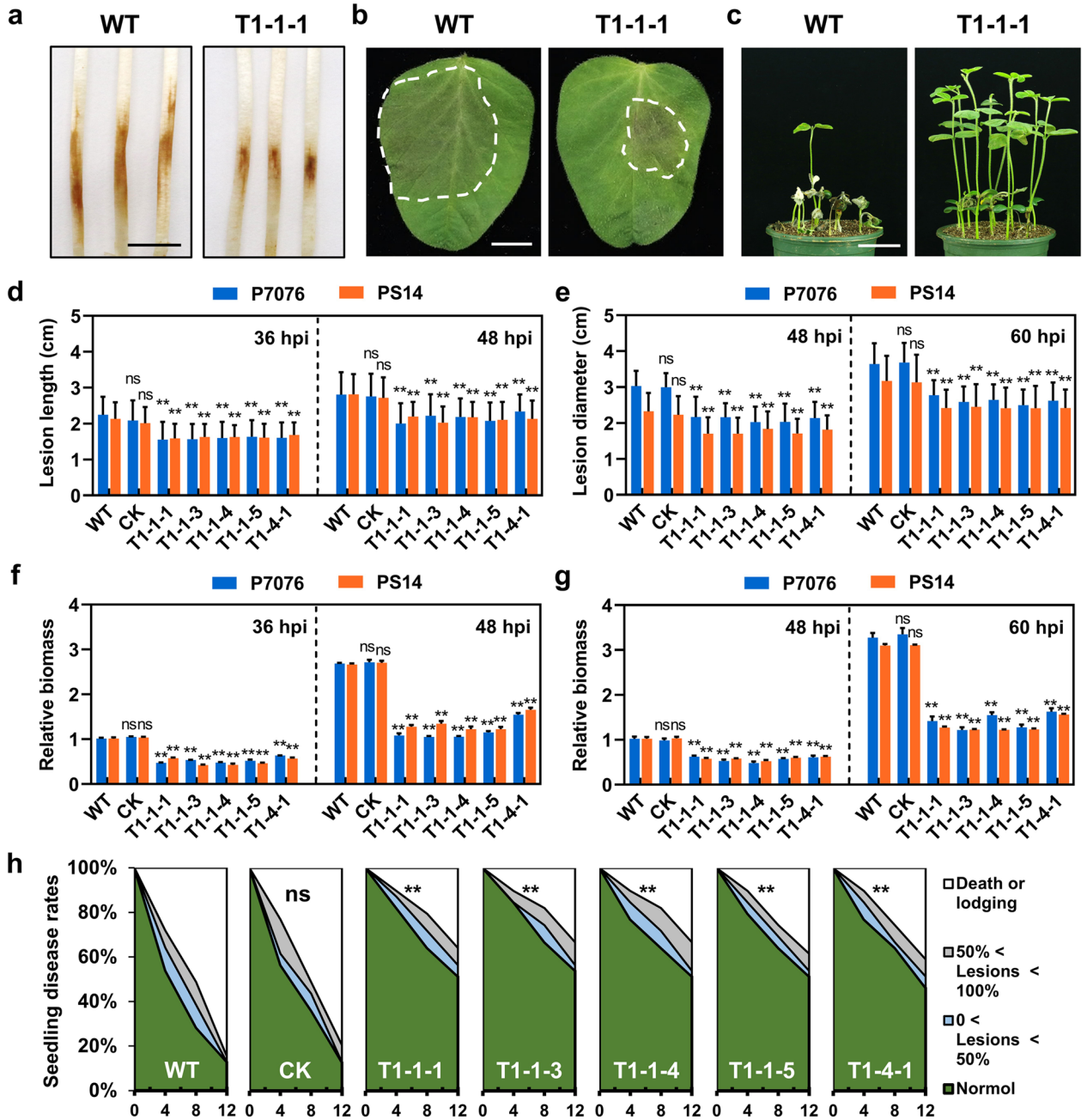


**Fig. 5** GmPAO significantly enhances resistance against *P. sojae* in the transgenic soybean lines. The soybean lines were the same as in Fig. 1. Two *P. sojae* isolates (P7076 and PS14) that are virulent on WT were used. **a**, **b** Representative disease phenotypes at 36 hpi (**a**) and 60 hpi (**b**). Hypocotyls or unifoliate leaves were inoculated with *P. sojae* P7076. Scale bars, 1 cm. **c** Representative disease phenotypes of seedlings at 12 dpi. The seedlings were inoculated with *P. sojae* P7076 ($5 \times 10^4$ zoospores/mL) using the root-dipping inoculation method. Scale bar, 5 cm. **d**, **e** Comparisons of the hypocotyl lesion lengths and leaf lesion diameters caused by *P. sojae* P7076 or *P. sojae* PS14. Error bar represents mean ± SD, n ≥ 12, n represents sample number. **f**, **g** Quantitation of resistance levels via assessment of *P. sojae* biomass accumulations in inoculated hypocotyls and leaves by genomic qPCR. Error bar represents mean ± SD, n = 3, n represents sample number. **h** Seedling disease ratings in the transgenic lines over time. The disease symptoms were recorded at 4, 8, and 12 dpi. Disease ratings are shown with different colors (n ≥ 12, n represents sample number). All the experiments were performed three times (biological replicates) with similar results. The data in **d**–**h** were analyzed by Shapiro–Wilk test to determine the Normality and Lognormality Tests across groups, and then analyzed by one-way ANOVA with post-hoc Dunnett's multiple comparisons test for groups that had passed the normality test (ns, no significant difference; $^{**}P < 0.01$). The exact n, SD values, and *P* values are shown in the data

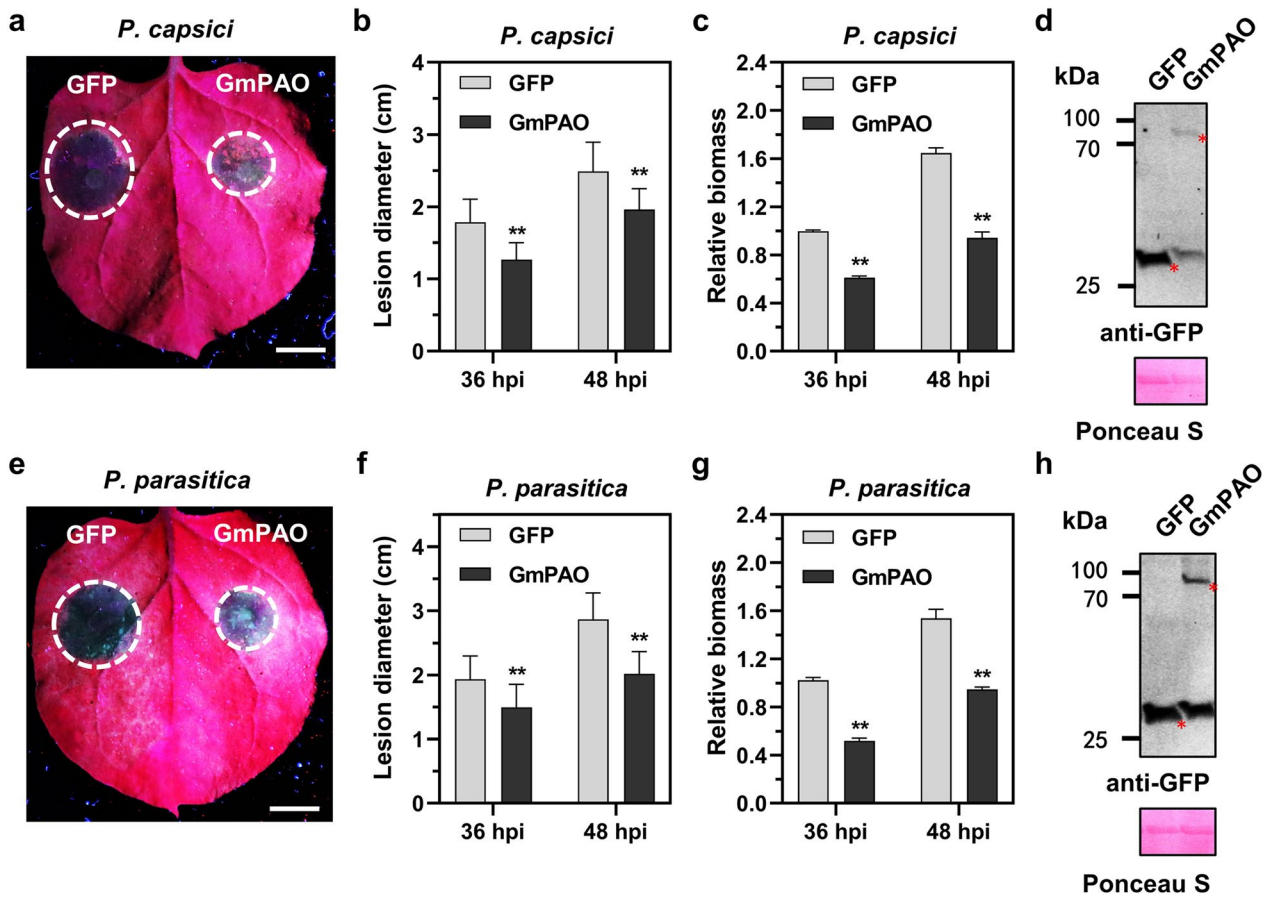


**Fig. 6** GmPAO enhances resistance to *P. capsici* and *P. parasitica* infections in *N. benthamiana*. **a**, **e** Lesions caused by *P. capsici* (**a**) or *P. parasitica* (**e**) on *N. benthamiana* leaves expressing *GFP* or *GmPAO* genes. *GFP* was used as a negative control. Photos were taken at 36 hpi. Scale bars, 1 cm. **b**, **f** Comparisons of the lesion diameter caused by *P. capsici* (**b**) or *P. parasitica* (**f**). Error bar represents mean ± SD, n ≥ 12, n represents sample number. **c**, **g** Relative pathogen biomass quantified by genomic qPCR. Error bar represents mean ± SD, n = 3, n represents sample number. **d**, **h** Representative immunoblot showing the levels of GFP and GmPAO after transient expression in *N. benthamiana* leaves. Proteins were stained with Ponceau S to confirm equal loading. All the experiments were performed three times (biological replicates) with similar results. The data in **b**, **c**, **f**, and **g** were analyzed by Shapiro–Wilk test to determine the Normality and Lognormality Tests across groups, and then analyzed by unpaired *t* test for groups that had passed the normality test (**$P < 0.01$). The exact n, SD values, and *P* values are shown in the data

## Discussion

*Phytophthora* pathogens cause destructive diseases in agricultural settings, thereby threatening global food security (Wang et al. 2020). Currently, selection and breeding of plant cultivars with broad-spectrum resistance are the most effective approaches for *Phytophthora* disease management. Compared with conventional breeding, genetic engineering can shorten breeding cycles and facilitate interspecific transfer of resistance genes (Zhou et al. 2021). However, few molecular breeding strategies have been designed to date for *Phytophthora* disease control or improvement of soybean disease resistance in general. Recent studies showed that $H_2O_2$ can be generated via Spd and Spm oxidation catalyzed by PAO (Moschou et al. 2009; Mo et al. 2015; Gerlin et al. 2021). Hence, we hypothesized that pathogen-enhanced production of plant Spd and Spm could be oxidized by overexpressed *GmPAO* to generate $H_2O_2$ and promote immunity responses, which are specific to pathogen infection but are not triggered in the absence of pathogen challenge.

Previous studies reported that during the interaction of wheat with *Fusarium graminearum*, the amount of Put in wheat plants increased rapidly while Spd slightly increased and Spm content did not change significantly (Ma et al. 2021). Another research reported that Spm and Put exhibited an increase of 2.5-fold and 2.0-fold, respectively, whereas Spd increased only slightly in the interaction of tobacco with *Pseudomonas syringae* (Moschou et al. 2009). Upon *P. sojae* infection, the amounts of Spd

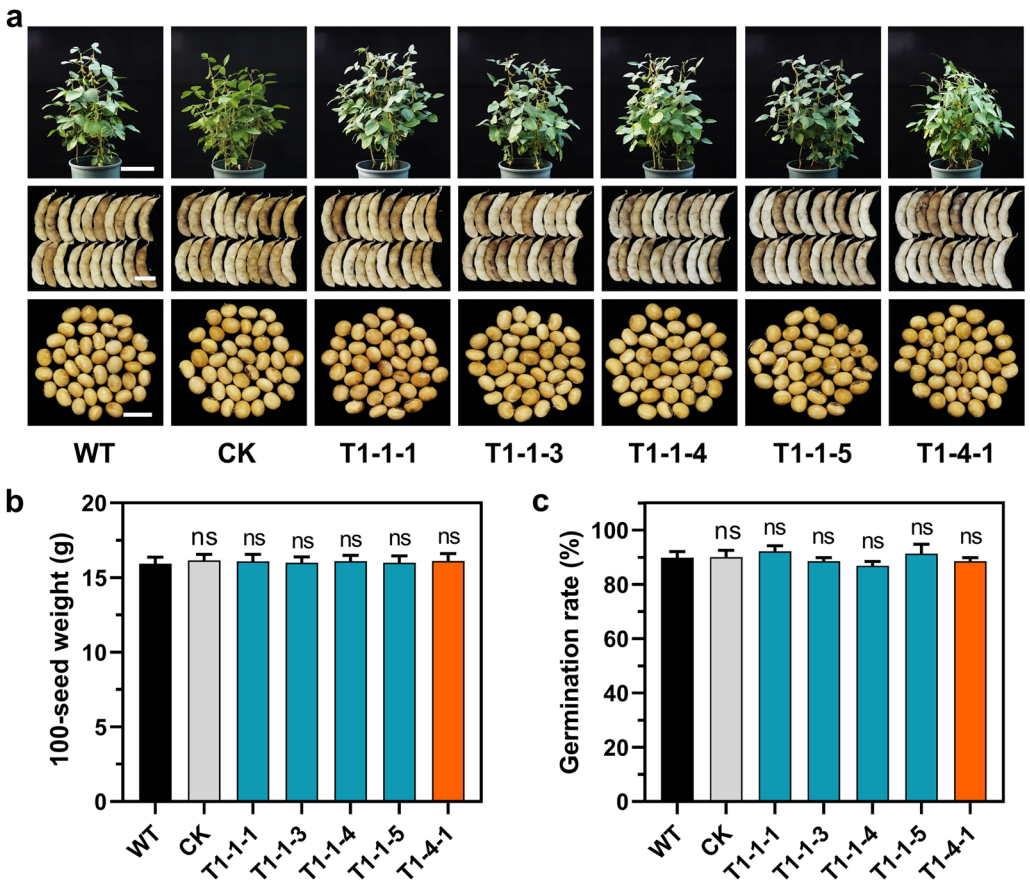


**Fig. 7** Agronomic traits of *GmPAO* overexpression soybean lines. The soybean lines were the same as in Fig. 1. **a** Growth phenotypes (upper) of soybean plants grown in growth chambers for two months. Scale bar, 20 cm. Pod (middle) and Seed (lower) morphology after harvest. Scale bars, 1 cm. **b** Statistical analysis of 100-seed weight of the transgenic soybean plants. The seeds were randomly chosen and weighed. Error bar represents mean ± SD, n = 20, n represents sample number. **c** Germination rate of the transgenic soybean plants. The number of germinated seeds was recorded after gemination for 8 days. Error bar represents mean ± SD, n = 3 experiments with 40 seeds. All the experiments were performed three times (biological replicates) with similar results. The data in **b** and **c** were analyzed by Shapiro–Wilk test to determine the Normality and Lognormality Tests across groups, and then analyzed by one-way ANOVA with post-hoc Dunnett's multiple comparisons test for groups that had passed the normality test (ns, no significant difference). The exact n, SD values, and *P* values are shown in the data

and Spm but not Put in soybean were increased (Fig. 1a). These PAs have been demonstrated to be catalyzed by PAO to generate $H_2O_2$ (Moschou et al. 2009; Seifi and Shelp 2019), which plays a central role in plant defense (Qi et al. 2017; Gao et al. 2021). Based on these results, we proposed that enhancement of Spd and Spm by pathogen infection could be used as targets to ensure pathogen-specific $H_2O_2$ generation by overexpressing *PAO*.

Here, we have shown that GmPAO could significantly enhance $H_2O_2$ content in transgenic soybean lines (Fig. 1d). Moschou et al. (2009) found that overexpression of maize *PAO* in *Nicotiana* increased $H_2O_2$ level. In another example, overexpression of cotton *PAO* in *Arabidopsis* also increased $H_2O_2$ content compared to wild type (Mo et al. 2015). Interestingly, we also found that GmPAO-mediated $H_2O_2$ only occurred at the *P. sojae* infection sites (Fig. 1c), thus minimizing cellular damage caused by $H_2O_2$. Modulation of polyamine metabolism under biotic stress has attracted wide interest; however, the precise functions of these amines in plant defense response against pathogen attack are still poorly understood. Recent studies have demonstrated that plant polyamines are involved in PTI against pathogens (Gerlin et al. 2021). Our results showed that GmPAO-mediated polyamine catabolism promoted flg22/chitin-induced $H_2O_2$ accumulation (Fig. 2), indicating that GmPAO can also promote PTI. In this disease resistance strategy, GmPAO-mediated $H_2O_2$ accumulation can improve plant resistance, and GmPAO-promoted PTI can further improve plant resistance (Fig. 8).

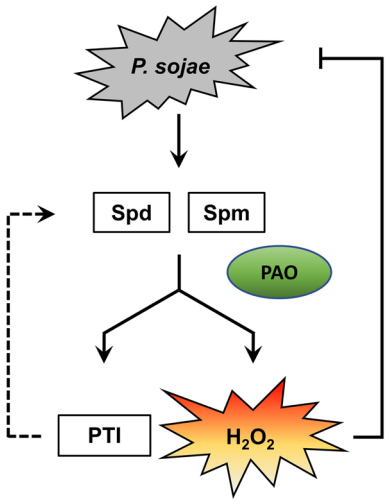


**Fig. 8** A proposed model illustrating the mechanism of GmPAO-mediated resistance. The two substrates Spd and Spm are increased upon *P. sojae* infection. GmPAO-mediated Spd/Spm catabolism enhances $H_2O_2$ production and PTI activation, thereby controlling the infection caused by *P. sojae*. The activation of PTI response might promote the increase of Spd and Spm contents in soybean

Our results indicated that all the transgenic soybean plants showed higher accumulations of Spd and Spm compared with WT and CK (Fig. 3). This is likely to be a feedback regulation that promotes the accumulation of Spd and Spm in soybean and/or a response of PTI activation (Fig. 8). An interesting question, what is the effect of increased Spd and Spm in soybean on the control of *P. sojae*? Our results indicated that high concentrations of Spd and Spm could inhibit *P. sojae*, but the concentrations of Spd and Spm in the transgenic lines were far below the inhibitory concentrations. Thus, the increased Spd and Spm in *GmPAO* overexpression soybean lines may boost $H_2O_2$ generation during interaction with pathogens, rather than direct inhibition of *P. sojae* (Fig. 8).

It has long been established that plants respond to pathogen attack with a transient burst of ROS and that ROS play a central role in plant immune responses (Qi et al. 2017). Meanwhile, ROS are widely produced in different cellular compartments under both biotic and abiotic stress conditions (Qi et al. 2017). Therefore, disease resistance induced by PAO-mediated $H_2O_2$ production tends to be durable and broad-spectrum. In this study, GmPAO enhanced resistance against *P. sojae* isolates P7076 and PS14 in the transgenic soybean lines (Fig. 5). Furthermore, we also showed that GmPAO improved *N. benthamiana* resistance to *P. capsici* and *P. parasitica* in agroinfiltration assays (Fig. 6), demonstrating its effectiveness in conferring broad-spectrum resistance. In addition, we measured the agronomic traits of transgenic soybean lines and found no negative effects (Fig. 7). In many cases, constitutively overexpressed transgenes adversely affected plant size and/or seed production. This study provides an approach to express the transgenes only when and where they are needed—at infection sites.

## Conclusions

In summary, we develop an efficient metabolic engineering strategy to promote soybean $H_2O_2$ production upon *Phytophthora* infection with no adverse impact on agronomic traits. Overexpression of *GmPAO* may confer broad-spectrum disease resistance by ensuring both PTI activation and $H_2O_2$ production specifically when and where *Phytophthora* pathogens are present.

## Methods

### Plasmid construction and generation of transgenic soybean lines

The sequence of *Glycine max* polyamine oxidase gene (Glyma.09G227500.1) was obtained from Phytozome databases. The recombinant constructs were introduced into cotyledonary explants of soybean (*Glycine max*) cultivar Williams 82 by *Agrobacterium*-mediated transformation (Wang et al. 2020). Soybean transformants were selected using herbicide with glufosinate-ammonium (50 mg/L) as the active ingredient (Bayer CropScience, Research Triangle Park, NC, USA). Transformants were allowed to self-pollinate in growth chamber. After five generations of herbicide selection, T5 homozygous lines were used for the experiments (Lin et al. 2016). Genomic DNA was extracted from leaves of putative transgenic plants and WT. Total RNA was extracted using an RNA-Simple Total RNA Kit (Tiangen, China) according to the manufacturer's instructions. Soybean cDNAs were synthesized using the Super-ScriptIII First-Strand Kit (Invitrogen, USA). Genomic PCR and quantitative PCR (qPCR) assays were used to screen and validate transgenic lines. *GmPAO*, selection gene (*Bar*), and internal reference (*ACT11*) were amplified using specific primers (Additional file 2: Table S2). All amplicons had the expected sizes.

### Plant materials, microbial strains, and growth conditions

Soybean cultivar Williams 82 was grown and maintained in plant growth chambers at an ambient temperature of 25 °C with a 16-h day/8-h night photoperiod. *N. benthamiana* plants were grown in soil in a plant growth chamber at 25 °C with 60% relative humidity and a 16 h light/8 h dark photoperiod. Two *P. sojae* isolates (P7076 and PS14) that are virulent to the soybean cultivar Williams 82 were used in this study. *P. sojae* isolates, *P. capsici* isolate LT263, and *P. parasitica* isolate 025 used in this

study were routinely cultured at 25 °C in the dark on 10% (v/v) V8 juice medium.

#### *Phytophthora* infection assays

*P. sojae* isolates (P7076 or PS14) that are virulent to Williams 82 were inoculated on soybean etiolated hypocotyls and leaves with mycelia, and seedlings by root-dipping method as described previously (Zhou et al. 2021). Lesion lengths or diameters were measured with the ImageJ software. Inoculated soybean seedlings were incubated for 12 days under controlled environmental conditions (25 °C, 16-h light/8-h dark photoperiod) before phenotypic scoring. The disease symptoms were recorded at 4, 8, and 12 dpi, and the disease rates were classified as no visible disease symptoms, < 50% of lesion areas, > 50% of lesion areas but still alive, and dead plants. The survival rate of WT, CK and transgenic soybean seedings at 12 dpi were statistically analyzed.

For the evaluation of disease resistance by transient expression, *N. benthamiana* leaves were agroinfiltrated with the binary vector pBIN4 (expressing *GFP*) on one-half of the leaf and the recombinant pBIN4 vector containing *GmPAO* was agroinfiltrated on the other half of the same leaf. The infiltrated leaves were inoculated with *P. capsici* or *P. parasitica* mycelia at 36 hpi. The lesion diameter was measured at 36/48 hpi, agroinfiltrated leaf samples were collected at 48 hpi and immediately frozen with liquid nitrogen before being stored for Western blot. For evaluation of disease development, relative quantification of *P. capsici* or *P. parasitica* biomass in infected leaves was performed by measuring the ratio of pathogen to host genomic DNA by qPCR as previously described (Zhou et al. 2021).

#### *Agrobacterium*-mediated transient gene expression

For transient expression assays, transformed *Agrobacterium* strains were cultured, washed, and resuspended in infiltration buffer (10 mM $MgCl_2$, 10 mM MES, and 150 μM acetosyringone) to make an appropriate optical density (OD) of 0.3 at 600 nm. Four-week-old *N. benthamiana* leaves were infiltrated with a 1:1 mixture of resuspended *Agrobacterium* containing the respective constructs and RNA silencing suppressor P19 (Li et al. 2019a).

#### SDS–PAGE and Western blot

Proteins from the sample lysate were fractionated by sodium dodecyl sulfate–polyacrylamide gel electrophoresis (SDS–PAGE). Fractionated proteins were electro-transferred from the gel to an Immobilon-PSQ polyvinylidene difluoride membrane using transfer buffer (20 mM Tris, 150 mM glycine). The membrane was then blocked for 30 min at room temperature using phosphate-buffered saline (PBS; pH 7.4) containing 3% nonfat dry milk with shaking at 50 rpm. After washing with PBST (PBS with 0.1% Tween 20), anti-HA (1:2000, Abmart) antibody was added to PBSTM (PBS with 0.1% Tween 20 and 3% nonfat dry milk) and incubated for 90 min. After three times of washing (5 min each) with PBST, the membrane was then incubated with goat anti-mouse IRDye 800CW antibody (Odyssey) at a ratio of 1:10,000 in PBSTM for 30 min. The membrane was finally washed with PBST and visualized with excitations at 700 and 800 nm (Yang et al. 2021).

#### The UHPLC-MS analysis of PAs

The samples were analyzed by LC–MS system (G2-XS QTof, Waters). 2 μL solution was injected into the UPLC column (2.1 × 100 mm ACQUITY UPLC BEH C18 column containing 1.7 μm particles) with a flow rate of 0.4 mL/min. Buffer A consisted of 0.1% formic acid in water, and buffer B consisted of 0.1% formic acid in acetonitrile. The gradient was 5% Buffer B for 0.5 min, 5–95% Buffer B for 11 min, and 95% Buffer B for 2 min. Mass spectrometry was performed using electrospray source in positive ion mode with MS acquisition mode, with a selected mass range of 100–1200 m/z. The lock mass option was enabled using leucine-enkephalin (m/z 556.2771) for recalibration. The ionization parameters were as follows: 2.5 kV of capillary voltage, 40 V of sample cone, 120 °C of source temperature, and 800 °C of desolvation gas temperature. Data acquisition and processing were performed using Masslynx 4.1 (Mo et al. 2015).

#### PAO enzymatic activity and $H_2O_2$ content assays

The level of PAO activity in plant tissues was determined using the spectrophotometric method (Mo et al. 2015). PAO activity was analyzed with a polyamine oxidase assay kit (Cominbio, China) according to the manufacturer's instructions. Soybean leaves were stained with 1 mg/mL DAB solution for 8 h in the dark at 16 hpi and then decolored with ethanol for light microscopy examination. Samples were equilibrated with 70% (v/v) glycerol for photography using natural light. $H_2O_2$ content was analyzed with a $H_2O_2$ assay kit (Beyotime Biotechnology, China) according to the manufacturer's instructions.

#### ROS production assay

Microbial pattern-triggered ROS burst assays were performed according to a previous report (Wang et al. 2020) with modifications. In brief, leaf disks were collected from 10-day-old soil-grown soybean plants or 4- to 5-week-old *N. benthamiana* plants and were incubated in water for 12 h in a 96-well plate. For ROS measurement in *N. benthamiana* plants, the indicated constructs

were transiently expressed in leaves by *Agrobacterium*-mediated transient expression for 2 days before cutting the leaf disks. The samples were treated with detection buffer, containing 20 μg/mL horseradish peroxidase (Sigma), 20 μM L-012 (Waco), and 1 μM flg22 (Sangon) or 200 μg/mL chitin (Sigma). Light emission was measured at 3-min intervals.

### Statistical analysis

Statistical analysis was performed using GraphPad Prism 8.3.0. Shapiro–Wilk test was used to determine normality and lognormality across groups. Groups passing the normality test were compared by unpaired *t* test or one-way ANOVA with post-hoc Dunnett's test for multiple comparisons (ns, no significant difference; $^{*}P < 0.05$; $^{**}P < 0.01$). Results are means ± SD.

#### Abbreviations

DAB: 3,3′-Diaminobenzidine; dpi: Days post-inoculation; ETI: Effector-triggered immunity; GmPAO: Soybean (*Glycine max*) polyamine oxidase; hpi: Hours post-inoculation; PAMP: Pathogen-associated molecular patterns; PAO: Polyamine oxidase; PAs: Polyamines; PTI: Pattern-triggered immunity; Put: Putrescine; ROS: Reactive oxygen species; Spd: Spermidine; Spm: Spermine; UHPLC-MS: Ultra-high-performance liquid chromatography coupled to quadrupole Orbitrap high-resolution mass spectrometry.

## Supplementary Information

The online version contains supplementary material available at https://doi.org/10.1186/s42483-022-00139-9.

**Additional file 1: Figure S1.** Molecular verification of transgenic soybean lines. **Figure S2.** Effects of PAs (Spd and Spm) on the pathogenicity of *P. sojae*. **Figure S3.** Disease phenotypes on hypocotyls of the transgenic soybean plants challenged with *P. sojae* P7076 (upper) or PS14 (lower) at 36 hpi. **Figure S4.** Disease phenotypes on unifoliate leaves of the transgenic soybean plants challenged with *P. sojae* P7076 (upper) or PS14 (lower) at 60 hpi. **Figure S5.** Disease phenotypes on seedlings of the transgenic soybean plants challenged with *P. sojae* at 12 dpi.

**Additional file 2: Table S1.** Statistical table of material identification for transgenic soybean lines. **Table S2.** Primers used in this study.

#### Acknowledgements

Not applicable.

#### Authors' contributions

DD conceived the project. KY, QY, and YW performed the experiments. KY, HP, MJ, and DD wrote the manuscript. All authors read and approved the final manuscript.

#### Funding

This work was supported by the National Natural Science Foundation of China (31721004 and 32072507).

#### Availability of data and materials

The datasets used and/or analyzed during the current study are available from the corresponding author on reasonable request.

## Declarations

#### Ethics approval and consent to participate

Not applicable.

#### Consent for publication

Not applicable.

#### Competing interests

The authors declare that they have no competing interests.

#### Author details

[1]Key Laboratory of Plant Immunity, College of Plant Protection, Academy for Advanced Interdisciplinary Studies, Nanjing Agricultural University, Nanjing 210095, China. [2]Institute of Industrial Crops, Jiangsu Academy of Agricultural Sciences/Jiangsu Key Laboratory for Horticultural Crop Genetic Improvement, Nanjing 210095, China. [3]Department of Plant Pathology, Washington State University, Pullman, WA 99164, USA.

Received: 30 May 2022 Accepted: 4 September 2022
Published online: 16 September 2022

#### References

Deng Y, Ning Y, Yang DL, Zhai K, Wang GL, He Z. Molecular basis of disease resistance and perspectives on breeding strategies for resistance improvement in crops. Mol Plant. 2020;13:1402–19. https://doi.org/10.1016/j.molp.2020.09.018.

Frailie TB, Innes RW. Engineering healthy crops: molecular strategies for enhancing the plant immune system. Curr Opin Biotechnol. 2021;70:151–7. https://doi.org/10.1016/j.copbio.2021.04.006.

Gao M, He Y, Yin X, Zhong X, Yan B, Wu Y, et al. $Ca^{2+}$ sensor-mediated ROS scavenging suppresses rice immunity and is exploited by a fungal effector. Cell. 2021;184(5391–404):e17. https://doi.org/10.1016/j.cell.2021.09.009.

Gerlin L, Baroukh C, Genin S. Polyamines: double agents in disease and plant immunity. Trends Plant Sci. 2021;26:1061–71. https://doi.org/10.1016/j.tplants.2021.05.007.

Jones JD, Dangl JL. The plant immune system. Nature. 2006;444:323–9. https://doi.org/10.1038/nature05286.

Kamoun S, Furzer O, Jones JD, Judelson HS, Ali GS, Dalio RJ, et al. The Top 10 oomycete pathogens in molecular plant pathology. Mol Plant Pathol. 2015;16:413–34. https://doi.org/10.1111/mpp.12190.

Kerchev PI, Van Breusegem F. Improving oxidative stress resilience in plants. Plant J. 2022;109:359–72. https://doi.org/10.1111/tpj.15493.

Koseoglou E, van der Wolf JM, Visser RGF, Bai Y. Susceptibility reversed: modified plant susceptibility genes for resistance to bacteria. Trends Plant Sci. 2022;27:69–79. https://doi.org/10.1016/j.tplants.2021.07.018.

Lamour KH, Stam R, Jupe J, Huitema E. The oomycete broad-host-range pathogen *Phytophthora capsici*. Mol Plant Pathol. 2012;13:329–37. https://doi.org/10.1111/j.1364-3703.2011.00754.x.

Li Q, Ai G, Shen DY, Zou F, Wang J, Bai T, et al. A *Phytophthora capsici* effector targets ACD11 binding partners that regulate ROS-mediated defense response in *Arabidopsis*. Mol Plant. 2019a;12:565–81. https://doi.org/10.1016/j.molp.2019.01.018.

Li Q, Chen YY, Wang J, Zou F, Jia YL, Shen DY, et al. A *Phytophthora capsici* virulence effector associates with NPR1 and suppresses plant immune responses. Phytopathol Res. 2019b;1:6. https://doi.org/10.1186/s42483-019-0013-y.

Li Q, Wang B, Yu J, Dou D. Pathogen-informed breeding for crop disease resistance. J Integr Plant Biol. 2021;63:305–11. https://doi.org/10.1111/jipb.13029.

Lin J, Mazarei M, Zhao N, Hatcher CN, Wuddineh WA, Rudis M, et al. Transgenic soybean overexpressing *GmSAMT1* exhibits resistance to multiple-HG types of soybean cyst nematode *Heterodera glycines*. Plant Biotechnol J. 2016;14:2100–9. https://doi.org/10.1111/pbi.12566.

Liu X, Ao K, Yao J, Zhang Y, Li X. Engineering plant disease resistance against biotrophic pathogens. Curr Opin Plant Biol. 2021;60:101987. https://doi.org/10.1016/j.pbi.2020.101987.

Ma H, Chen J, Zhang Z, Ma L, Yang Z, Zhang Q, et al. MAPK kinase 10.2 promotes disease resistance and drought tolerance by activating different MAPKs in rice. Plant J. 2017;92:557–70. https://doi.org/10.1111/tpj.13674.

Ma T, Zhang L, Wang M, Li Y, Jian Y, Wu L, et al. Plant defense compound triggers mycotoxin synthesis by regulating H2B ub1 and H3K4 me2/3 deposition. New Phytol. 2021;232:2106–23. https://doi.org/10.1111/nph.17718.

Mittler R. ROS are good. Trends Plant Sci. 2017;22:11–9. https://doi.org/10.1016/j.tplants.2016.08.002.
Mo HJ, Wang XF, Zhang Y, Zhang GY, Zhang JF, Ma ZY. Cotton polyamine oxidase is required for spermine and camalexin signalling in the defence response to *Verticillium dahliae*. Plant J. 2015;83:962–75. https://doi.org/10.1111/tpj.12941.
Moschou PN, Sarris PF, Skandalis N, Andriopoulou AH, Paschalidis KA, Panopoulos NJ, et al. Engineered polyamine catabolism preinduces tolerance of tobacco to bacteria and oomycetes. Plant Physiol. 2009;149:1970–81. https://doi.org/10.1104/pp.108.134932.
Narvaez I, Pliego Prieto C, Palomo-Rios E, Fresta L, Jimenez-Diaz RM, Trapero-Casas JL, et al. Heterologous expression of the *AtNPR1* gene in olive and its effects on fungal tolerance. Front Plant Sci. 2020;11:308. https://doi.org/10.3389/fpls.2020.00308.
Ning Y, Liu W, Wang GL. Balancing immunity and yield in crop plants. Trends Plant Sci. 2017;22:1069–79. https://doi.org/10.1016/j.tplants.2017.09.010.
Panabieres F, Ali GS, Alagui MB, Dalio RJD, Gudmestad NC, Kuhn ML, et al. *Phytophthora nicotianae* diseases worldwide: new knowledge of a long-recognised pathogen. Phytopathol Mediterr. 2016;55:20–40. https://doi.org/10.14601/Phytopathol_Mediterr-16423.
Pi L, Yin Z, Duan W, Wang N, Zhang Y, Wang J, et al. A G-type lectin receptor-like kinase regulates the perception of oomycete apoplastic expansin-like proteins. J Integr Plant Biol. 2022;64:183–201. https://doi.org/10.1111/jipb.13194.
Qi J, Wang J, Gong Z, Zhou JM. Apoplastic ROS signaling in plant immunity. Curr Opin Plant Biol. 2017;38:92–100. https://doi.org/10.1016/j.pbi.2017.04.022.
Qi J, Song CP, Wang B, Zhou J, Kangasjarvi J, Zhu JK, et al. Reactive oxygen species signaling and stomatal movement in plant responses to drought stress and pathogen attack. J Integr Plant Biol. 2018;60:805–26. https://doi.org/10.1111/jipb.12654.
Seifi HS, Shelp BJ. Spermine differentially refines plant defense responses against biotic and abiotic stresses. Front Plant Sci. 2019;10:117. https://doi.org/10.3389/fpls.2019.00117.
Sinha R, Shukla P. Antimicrobial peptides: recent insights on biotechnological interventions and future perspectives. Protein Pept Lett. 2019;26:79–87. https://doi.org/10.2174/0929866525666181026160852.
Tian J, Xu G, Yuan M. Towards engineering broad-spectrum disease-resistant crops. Trends Plant Sci. 2020;25:424–7. https://doi.org/10.1016/j.tplants.2020.02.012.
Wang DM, Liang XX, Bao YZ, Yang SX, Zhang X, Yu H, et al. A malectin-like receptor kinase regulates cell death and pattern-triggered immunity in soybean. Embo Rep. 2020;21:50442. https://doi.org/10.15252/embr.202050442.
Wang J, Zhou L, Shi H, Chern M, Yu H, Yi H, et al. A single transcription factor promotes both yield and immunity in rice. Science. 2018;361:1026–8. https://doi.org/10.1126/science.aat7675.
Xu G, Yuan M, Ai C, Liu L, Zhuang E, Karapetyan S, et al. uORF-mediated translation allows engineered plant disease resistance without fitness costs. Nature. 2017;545:491–4. https://doi.org/10.1038/nature22372.
Yang K, Dong X, Li J, Wang Y, Cheng Y, Zhai Y, et al. Type 2 Nep1-like proteins from the biocontrol oomycete *Pythium oligandrum* suppress *Phytophthora capsici* infection in solanaceous plants. J Fungi. 2021;7:496. https://doi.org/10.3390/jof7070496.
Yin Y, Wang Z, Cheng D, Chen X, Chen Y, Ma Z. The ATP-binding protein FgArb1 is essential for penetration, infectious and normal growth of *Fusarium graminearum*. New Phytol. 2018;219:1447–66. https://doi.org/10.1111/nph.15261.
Yu J, Chai CY, Ai G, Jia YL, Liu WJ, Zhang X, et al. A *Nicotiana benthamiana* AP2/ERF transcription factor confers resistance to *Phytophthora parasitica*. Phytopathol Res. 2020;2:4. https://doi.org/10.1186/s42483-020-0045-3.
Zhang C, Gao H, Li R, Han D, Wang L, Wu J, et al. GmBTB/POZ, a novel BTB/POZ domain-containing nuclear protein, positively regulates the response of soybean to *Phytophthora sojae* infection. Mol Plant Pathol. 2019a;20:78–91. https://doi.org/10.1111/mpp.12741.
Zhang X, Liu B, Zou F, Shen D, Yin Z, Wang R, et al. Whole genome re-sequencing reveals natural variation and adaptive evolution of *Phytophthora sojae*. Front Microbiol. 2019b;10:2792. https://doi.org/10.3389/fmicb.2019.02792.
Zhou Y, Yang K, Yan Q, Wang X, Cheng M, Si J, et al. Targeting of anti-microbial proteins to the hyphal surface amplifies protection of crop plants against *Phytophthora* pathogens. Mol Plant. 2021;14:1391–403. https://doi.org/10.1016/j.molp.2021.05.007.